Int. J. Heat Mass Transfer. Vol. 22, pp. 137–149

0017-9310/79/0101-0137 $02.00/0

BUOYANCY INDUCED FLOWS ADJACENT TO HORIZONTAL SURFACES IN WATER NEAR ITS DENSITY EXTREMUM

BENJAMIN GEBHART,* MICHAEL S. BENDELL† and HUSSAIN SHAUKATULLAH*

(*Received* 23 *September* 1977 *and in revised form* 3 *February* 1978)

Abstract—Buoyancy induced flows generated in cold water adjacent to a horizontal surface are analyzed. A boundary region treatment is appropriate for a broad range of conditions when the net effect of the buoyancy force is away from the surface. This results in on-flow at a leading edge for a plane flow, which may arise when the spatial configuration of the buoyancy force may be described in two dimensional Cartesian coordinates. A radial or disk-flow results when the configuration is radially symmetric about a normal to the surface. The boundary-layer regime again results when the net buoyancy is away from the surface and flow is outward from the axis. Both kinds of thermally buoyant flows are considered in low temperature pure or saline water, wherein a density extremum may occur in the region of buoyancy. A new, very accurate and simple density equation yields a compact transport formulation for both plane and disk flows. Solutions are given for the Prandtl number and temperature conditions which normally occur. Buoyancy reversals and conditions for convective inversion arise. Detailed tabulations of transport parameters are included for both the isothermal and the uniform surface flux conditions. These results are compared with those arising when the conventional buoyancy force approximation is used.

NOMENCLATURE

a,b,c,d, defined in equations (8)–(10);
c_p, specific heat of water;
f, non-dimensional stream function;
f_1,f_2,f_3,f_4, coefficients in density equation (1);
G, modified Grashof number $= 5(Gr/5)^{1/5}$;
Gr, Grashof number;
g, acceleration due to gravity;
g_1,g_2,g_3,g_4, coefficients in density equation (1);
h_1,h_2,h_3,h_4, coefficients in density equation (1);
I_w, total buoyancy force, equation (24);
k, thermal conductivity;
n, defined in equation (16);
P, non-dimensional pressure;
p, pressure;
p_h, hydrostatic pressure;
p_m, motion pressure;
Q, total local convected energy;
q, exponent in density equation (1);
R, $= (t_m - t_\infty)/(t_0 - t_\infty)$;
s, salinity;
s_∞, salinity of ambient fluid;
t, temperature;
t_{il}, temperature of ice formation;
t_m, temperature where density is maximum;
t_0, surface temperature;
t_∞, ambient temperature;
u, tangential velocity component;
v, normal velocity component;
W, local buoyancy force;
x, distance along the surface;
y, distance normal to the surface.

Greek symbols

α, coefficient in density equation (1);
β, coefficient of thermal expansion;
δ, boundary region thickness;
η, non-dimensional distance in boundary region;
η_δ, value of η at the edge of boundary region;
ν, kinematic viscosity;
ρ, density;
ρ_m, maximum density;
ρ_∞, density of ambient fluid;
ϕ, non-dimensional temperature $= (t - t_\infty)/(t_0 - t_\infty)$;
ψ, stream function.

Superscript

$'$, differentiation with respect to η.

INTRODUCTION

BUOYANCY induced flows adjacent to horizontal or nearly horizontal surfaces have not been studied as extensively as those adjacent to vertical surfaces and in freely rising plumes. However, they are very important in many applications both in the environment and in technology. The flow which concerns us here is that which arises adjacent to a horizontal surface, in an extensive ambient medium, as a result of a surface temperature different from that of the ambient medium. Past observations of flows arising from isolated surfaces have shown the existence,

*State University of New York at Buffalo, Buffalo, New York 14214, U.S.A.
†Sunpower Inc., 48 West Union Street, Athens, Ohio 45701, U.S.A.

close to the surface, of a boundary-layer mode of convection, followed, after a region of instability, by a cellular motion. Schmidt [1] was apparently the first to experimentally investigate flow above a flat horizontal surface.

For thermal buoyancy alone, and the usual approximations concerning density levels and differences, often called the Boussinesq or conventional approximations, Stewartson [2] analyzed flow adjacent to a semi-infinite isothermal surface, that is, a surface with a single leading edge. A sign mistake in the analysis led to an erroneous conclusion regarding the necessary condition for the existence of a boundary-layer like flow adjacent to such a surface. This was corrected by Gill, Zeh and Del Casal [3] who showed that the necessary condition was that the buoyancy force be away from the surface, as for a heated surface facing upward or a cooled surface facing downward.

Rotem and Claassen [4, 5] obtained solutions for an isothermal surface for several specific values of Prandtl number. Asymptotic results for zero and infinite Prandtl numbers are also given in [4]. Experimental observations with a Schlieren system clearly indicated the existence of a boundary layer near the leading edge on the upper side of a heated horizontal surface, insulated on the bottom face. Rotem [6] and Rotem and Claassen [4] also formulated the similarity solution for horizontal axisymmetric boundary-layer flow adjacent to an unbounded horizontal surface and gave solutions for an isothermal surface condition for an unspecified Prandtl number. These are sometimes called disk flows, in contrast to the plane flows previously considered.

Pera and Gebhart [7] and [8] studied both flow and the stability of horizontal and slightly inclined plane flows. For a horizontal orientation, the experimental results in air indicated an attached region, with characteristics close to those predicted. This region was followed downstream by a flow separation in the form of very rapidly growing longitudinal vortices. This latter consequence, along with upstream disturbance growth characteristics, implied an initiating role for upstream two-dimensional spanwise disturbances.

Blanc and Gebhart [9] discuss, for disk flows, the limits of physical reasonableness of a variation of $t_0 - t_\infty$, i.e. the difference between the local surface and ambient medium temperatures. Solutions are given for both isothermal and uniform flux conditions, for t_∞ uniform. Then procedures are presented which give exact solutions of some disk and plane flows.

The present paper treats both the horizontal plane and the axisymmetric flows, generated in both pure and saline water, at temperature conditions which may result in density extrema in the convection region, e.g. at about 4°C at a pressure of 1 bar in pure water. Such flows are found in the melting and freezing of ice surfaces and in processing technology. Another very interesting and important mechanism in such a horizontal configuration is the penetrative convection which may arise in unstable stratification. For simplicity, that transport process will be separately treated.

A NEW DENSITY CORRELATION

For conditions around an extremum the conventional approximation which evaluates the buoyancy force $g(\rho_\infty - \rho)$ as $g\rho\beta(t - t_\infty)$, in a thermally driven flow, may not be used. See Gebhart and Mollendorf [10]. Other density information becomes necessary. From the importance of the properties of pure and saline water have followed, over many years, many investigations of density dependence on t, s and p. However, this collection of information was not developed for accuracy in the region of inversion. In addition, none of the available correlations are in a convenient form for analysis.

Gebhart and Mollendorf [11], have recently developed a much simpler density relation which gives very high accuracy around the inversion temperature, in the temperature range from phase equilibrium up to 20°C. It includes both pure and saline water and applies to 40 ppt ($^o/_{oo}$) salinity, s, and to 1000 bars pressure. The agreement with modern density data over this whole region is about 10 ppm (RMS). The relation is

$$\rho(t, s, p) = \rho_m(s, p)[1 - \alpha(s, p)|t - t_m(s, p)|^{q(s,p)}] \tag{1a}$$

where $\rho_m(s, p)$ is the maximum density at s and p, $t_m(s, p)$ is the corresponding inversion temperature and $q(s, p)$ is the exponent. Salinity is in parts per thousand, $^o/_{oo}$, and pressure is in bars, 1 atm $\approx$ 1.01 bars. The s and p dependent quantities above are expressed as follows:

$$\rho_m(s, p) = \rho_m(0, 1)[1 + f_1(p) + sg_1(p) + s^2h_1(p)] \tag{1b}$$

$$\alpha(s, p) = \alpha(0, 1)[1 + f_2(p) + sg_2(p) + s^2h_2(p)] \tag{1c}$$

$$t_m(s, p) = t_m(0, 1)[1 + f_3(p) + sg_3(p) + s^2h_3(p)] \tag{1d}$$

$$q(s, p) = q(0, 1)[1 + f_4(p) + sg_4(p) + s^2h_4(p)]. \tag{1e}$$

The functions f_i, g_i and h_i are the polynomials in $(p - 1)$ and are given in Gebhart and Mollendorf [11]. The $(0, 1)$ quantities are values for pure water at 1 bar abs. Of these, only $\rho_m(0, 1) = 999.972\,\mathrm{kg\,m^{-3}}$ was chosen. The other ones, along with the coefficients in the polynomials, were determined by a non-linear regression. Results are tabulated in [11] for the best fit and also for a much simpler one of sufficient accuracy for most analysis. Values of $\alpha(0, 1)$ and $t_m(0, 1)$ are $9.297173 \times 10^{-6}\,^\circ\mathrm{C}^{-q}$ and 4.029325°C respectively. The large number of digits in all coefficients result from fitting the equation to data at the level of ppm.

Note that equation (1) contains only a single term

in temperature, an expansion around the extremum temperature at the local conditions s and p. This simple dependence is extremely important in analysis. The simple salinity dependence is also very useful since salinity gradients are very much more important than pressure gradients in diffusive processes at the size scale of interest here. The above form results in very few additional parameters in a boundary-layer formulation.

The liquid phase in water is limited in equilibrium by the conditions of pressure, temperature and salinity at which a solid phase appears. The temperature of ice melting t_{il} was recently determined by Fujino, Lewis and Perkin [12] to be

$$t_{il}(s,p) = -0.02831 - 0.499s - 0.000112s^2 - 0.00759p \quad (2)$$

where p is in bars absolute. This is the form corrected through personal communication with Dr. E. L. Lewis.

Using this expression, in conjunction with $t_m(s,p)$ determined in our correlation, we find that the extremum occurs in pure water at pressures less than about 300 bars and for salinities of less than about 25‰ at 1 bar. However, our expression gives high accuracy well beyond these s and p limits. These and other relevant matters are discussed in more detail by Gebhart and Mollendorf [10] and [11].

ANALYSIS OF PLANE FLOW

Employing the first Boussinesq approximation in the mass continuity equation, the first-order boundary-layer equations, with no saline diffusion, are

$$u\frac{\partial u}{\partial x} + v\frac{\partial u}{\partial y} = \nu\frac{\partial^2 u}{\partial y^2} - \frac{1}{\rho}\frac{\partial p_m}{\partial x} \quad (3)$$

$$0 = -\frac{1}{\rho}\frac{\partial p_m}{\partial y} + \frac{g(\rho_\infty - \rho)}{\rho} \quad (4)$$

$$u\frac{\partial t}{\partial x} + v\frac{\partial t}{\partial y} = \frac{k}{\rho c_p}\frac{\partial^2 t}{\partial y^2} \quad (5)$$

$$\frac{\partial u}{\partial x} + \frac{\partial v}{\partial y} = 0 \quad (6)$$

where y is the vertical coordinate and u and v are velocity components parallel to the x and y directions. The static pressure p has been taken as the sum of the local hydrostatic pressure p_h and motion pressure p_m, ρ_m is some representative density level, k is thermal conductivity and c_p is specific heat. Gravitational acceleration, g, carries a sign, being positive if in the same direction as y and negative if in the opposite direction.

The buoyancy force is determined from (1) at a given level of s and p, where $\alpha = \alpha(s,p)$, $\rho_m = \rho_m(s,p)$, $t_m = t_m(s,p)$ and $q = q(s,p)$, as

$$\rho_\infty - \rho = \alpha\rho_m(|t - t_m|^q - |t_\infty - t_m|^q). \quad (7)$$

With the usual stream function, we use the following transformation to seek similarity,

$$\eta(x,y) = b(x)y, \quad \psi(x,y) = \nu c(x) f(\eta) \quad (8)$$

$$\phi(\eta) = \frac{t - t_\infty}{t_0 - t_\infty} = \frac{t - t_\infty}{\mathrm{d}(x)} \quad (9)$$

$$p_m = a(x)P(\eta) \quad (10)$$

$$R = \frac{t_m(s,p) - t_\infty}{t_0 - t_\infty}. \quad (11)$$

Introducing (9) and (11) into (1) we evaluate the buoyancy force W.

$$\rho_\infty - \rho = \alpha\rho_m|t_0 - t_\infty|^q(|\phi - R|^q - |R|^q) = \alpha\rho_m|t_0 - t_\infty|^q W. \quad (12)$$

Introducing the transformation into (3)–(6) we obtain

$$f''' + \frac{c_x}{b}ff'' - \left(\frac{c_x}{b} + \frac{cb_x}{b^2}\right)f'^2 - \frac{1}{\rho\nu^2}\left(\frac{a_x}{cb^3}P + \frac{ab_x}{cb^4}\eta P'\right) = 0 \quad (13)$$

$$P' = -\frac{g\alpha\rho_m}{ab}|t_0 - t_\infty|^q(|\phi - R|^q - |R|^q) = -\frac{g\alpha\rho_m}{ab}|t_0 - t_\infty|^q W \quad (14)$$

$$\phi'' + Pr\left[\frac{c_x}{b}f'\phi' - \frac{cd_x}{db}\phi f'\right] = 0. \quad (15)$$

For similarity, all the coefficients in the above equations must be constants or functions of η only. Similarity may arise either for an exponential or for a power law dependence in $d(x)$. Taking the power law variation

$$d(x) = t_0 - t_\infty = Nx^n \quad (16)$$

and choosing the reference density as ρ_m, we find

$$c = G \quad (17)$$

$$b = G/5x \quad (18)$$

$$a = \frac{\nu^2\rho}{125x^2}(G)^4 \quad (19)$$

where

$$G = 5\left(\frac{Gr_x}{5}\right)^{1/5} = 5\left(\frac{gx^3}{5\nu^2}\alpha|t_0 - t_\infty|^q\right)^{1/5} = 5\left(\frac{g\alpha N^q x^{3+nq}}{5\nu^2}\right)^{1/5}. \quad (20)$$

The Grashof number Gr_x in (20) characterizes such flows. However, as we shall see, it is not in general an accurate indicator of either the vigor of the local flow or of its detailed directional tendencies under all conditions involving extrema. Note that it

is always positive, given the definition of x. In terms of the above quantities the differential equations become

$$f''' + (nq+3)ff'' - (2nq+1)f'^2 - \frac{4nq+2}{5}P - \frac{nq-2}{5}\eta P' = 0 \quad (21)$$

$$P' = -\text{sign}(g)(|\phi - R|^q - |R|^q) = -\text{sign}(g)W \quad (22)$$

$$\phi'' + Pr[(nq+3)f\phi' - 5n\phi f'] = 0. \quad (23)$$

The variations of $\rho_m(s,p)$, $\alpha(s,p)$, $t_m(s,p)$ and $q(s,p)$ in flow regions of limited vertical extent are negligible, in the absence of saline diffusion, to the order of approximation seen, for example, in (3)–(6). Thus, s and p merely determine single values of ρ_m, α, t_m and q over the flow field. We note that any imposed variation of t_∞ or s_∞ with x may result in a variation of $\rho_\infty(s,p)$. This would result in motion in the ambient medium, analogous to baroclinic motion. This possibility we exclude by taking both t_∞ and s_∞ uniform. Therefore, the only remaining x dependence of (22) is possibly due to R.

From (14) it is seen that any purely x dependence of R may not be removed by transformation of W, since $\phi = \phi(\eta)$ with similarity. Thus, the necessary conditions for similarity are either $R = 0 (t_\infty = t_m)$ or $t_0 - t_\infty$ independent of x (t_0 is uniform). Therefore, there is similarity in $W = W(\eta, R)$ either for R being zero or a constant.

For a horizontal surface, there is no component of buoyancy force parallel to the surface. The flow is driven entirely by a favorable motion pressure gradient, ∇P, arising through the buoyancy force, W in equation (22). The total buoyancy force across the boundary region is given by

$$I_w = \int_0^\infty W\,d\eta = \int_0^\infty (|\phi - R|^q - |R|^q)\,d\eta. \quad (24)$$

This quantity gives an estimate of the vigor of flow. It could have been incorporated into the definition of the Grashof number, in (20). The sign of I_w is also important and is discussed below.

Limits on the applicability of this formulation may now be determined from the total local convected energy $Q(x)$, the local boundary region thickness $\delta(x)$ and the pressure gradient $\partial p_m/\partial x$. These are

$$Q(x) = \int_0^\infty \rho c_p (t - t_\infty) u\,dy \propto x^{[(5+q)n+3]/5} \quad (25)$$

$$\delta(x) = \frac{\eta_\delta}{b} \propto x^{(2-nq)/5} \quad (26)$$

$$\frac{\partial p_m}{\partial x} = \text{sign}(g)\frac{\nu^2\rho}{x^3}\left(\frac{g\alpha x^3 d^q}{5\nu^2}\right)^{4/5} \times \left[(4nq+2)\int_\eta^\infty W\,d\eta + (2-nq)\eta W\right]. \quad (27)$$

The integrated value of pressure gradient across the flow region is

$$\int_0^\infty \frac{\partial p_m}{\partial x}dy = \text{sign}(g)\frac{\nu^2\rho}{x^4}\left[\frac{g\alpha x^3 d^q}{5\nu^2}\right] \times \left[(4nq+2)\int_0^\infty \int_\eta^\infty W\,d\eta_1\,d\eta + (2-nq)\eta I_w\right]. \quad (28)$$

For a heated or a cooled surface, $|Q(x)|$ must always increase with x or, in the limit, remain constant. Therefore, from (25), $n \geq -3/(5+q)$. From (26), for $\delta(0) = 0$, $n < 2/q$. From (27) and (28) it is seen that the sign of pressure gradient depends on the sign of g, W and I_w. From the definition of W it can easily be shown, by plotting W vs ϕ, that for $R \leq 0$, W and, therefore, I_w, are always positive. For $R \geq 0.5$, W and I_w are always negative. Therefore, the sign of the pressure gradient will be negative for $-1/2q \leq n \leq 2/q$, see (27) and (28), for $R \leq 0$, if the sign of g is negative. This is flow on the upper side. For $R \geq 0.5$ and positive g, on-flow results on the bottom side of the surface.

In the region $0 < R < 0.5$, W changes sign across the boundary region and there is no way to tell *a priori* what value of R would produce a developing boundary-layer-regime flow in the positive x direction, above or below a surface. The final resolution of this question lies in the complicated interaction of buoyancy with momentum level and with thermal and momentum diffusion. There is some very indirect guidance in the experiments of Dumoré *et al.* [13] and of Schenk and Schenkels [14], both with spheres of ice in water. An apparent "convective inversion" occurred at value of the present R of 0.17 and 0.25, respectively. The recent results of Bendell and Gebhart [15], with a vertical ice surface in water, determined that the inversion occurred at a value of R between 0.27 and 0.28. Consider, for example, a slab of ice, at 0°C throughout, bounded below by fresh water, at atmospheric pressure. Then $t_0 = 0$°C. The solid curve in Fig. 1 is the density distribution vs temperature, t/t_m, out toward the ambient condition. Also shown are values of R when t is taken as t_∞, i.e. for varying ambient temperature. For $t_\infty \leq t_m$ i.e. $R \leq 0$, the buoyancy force W is upward over the whole convective layer, from t_0 to t_∞. However, for $t_\infty > t_m$ there are regions in the outer part of the region, where the local buoyancy force is down. This reversal region increases with an increase in R until, at $R = 0.5$, the buoyancy force is downward across the whole region. For larger t_∞ (or R), the local buoyancy force is everywhere down. The local buoyancy force W is related to the changing motion pressure by equation (22).

There are many interesting and important applications to consider. We treat two classes here. The first is $t_0 - t_\infty$ = constant, ($n = 0$). This includes the melting of an ice slab for the characteristic range of R values seen in Fig. 1. It also includes consideration of transport for additional values of R when $t_0 \neq 0$°C. The above formulation (21)–(23), is general.

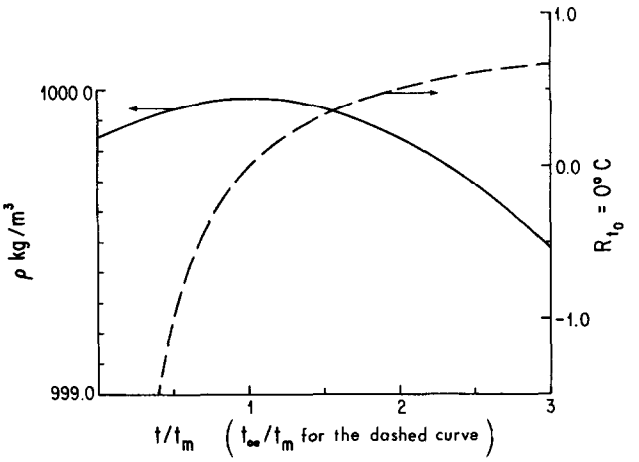

FIG. 1. Density variation of pure water at 1 bar. Dashed curve gives values of R for an ice surface at 0°C, i.e. $t_0 = 0$°C.

Another interesting circumstance considered is that of a surface dissipating heat uniformly, i.e. $q''(x)$ = constant. Thus $Q(x) \propto x$. This is seen in (25) to result when $n = 2/(q+5)$. For $q(0, 1)$ we have $n = 0.2901$. This condition includes applications which might arise in radiation or other heat flux loading of a surface in contact with cold water. In general, the results of primary interest are the heat transfer and viscous drag parameters, $-\phi'(0)$ and $f''(0)$. The local Nusselt number is calculated from the former as

$$Nu_x = -\phi'(0)\left(\frac{gx^3\alpha|t_0 - t_\infty|^q}{5\nu^2}\right)^{1/5}. \quad (29)$$

Also of particular interest are the conditions under which buoyancy force reversals across the flow region might result in the net buoyancy force I_w becoming very small and perhaps changing sign. This possibility was seen in the particular example above of $t_0 = 0$°C as t_∞ decreases from high values toward t_m, R decreases from the asymptotic value of 1.0. The fluid in the convective region is at first everywhere more dense than in the ambient medium, a downward buoyancy force, negative W. This means on-flow on the lower side of a horizontal surface. However, for $t_\infty < 2t_m$, the buoyancy force W becomes increasingly positive in the region adjacent to the surface. This region increases in extent as t_∞ decreases and, although I_W is still negative, it approaches zero.

On the other hand, if $t_\infty = t_m$, then W is positive over the whole convective region and, $I_W > 0$. This is on-flow on the upper side of a horizontal surface. It is seen that for t_∞ taken successively higher than t_m, I_W decreases again toward zero, due to an increasing negative contribution to net buoyancy in the outer part of the convective region. Therefore, there is a value of R, or perhaps some range of values of R around $I_W = 0$, for which no reasonable solution may be expected. Convective inversion lies somewhere in this range.

Recall that $t_0 = 0$°C has only been chosen as a specific example to demonstrate the mechanisms which arise through the buoyancy reversals encountered around t_m. Other choices of t_0 lead to similar results as t_∞ takes on different values with respect of the particular value of $t_m(s, p)$ which applies.

CALCULATIONS FOR AN ISOTHERMAL SURFACE CONDITION

It is apparent that the local buoyancy force changes direction somewhere across the flow region throughout the range $0 < R < 1/2$. The calculations were carried out on both sides of this region and into it from above, toward the inversion condition. The equations, (21)–(23), and boundary conditions, with $n = 0$, are

$$f''' + 3f''f - f'^2 + \tfrac{2}{5}P'\eta - \tfrac{2}{5}P = 0 \quad (30)$$

$$P' = W = |\varphi - R|^q - |R|^q \quad (31)$$

$$\varphi + 3Pr\varphi' f = 0 \quad (32)$$

$$f(0) = f'(0) = 1 - \varphi(0) = \varphi(\infty) = f'(\infty) = p(\infty) = 0. \quad (33)$$

These were solved for characteristic values of the Prandtl number at low temperatures, 10.6, 11.6 and 12.6, and with $q = q(0, 1) = 1.894816$ and $q(0,1000) = 1.58295$. The values of R of 16, 8, 4, 2, 1, 0.5, and 0.301 amount to flow along the bottom side of the surface. Calculations were also made for R of -16, -8, -4, -2, -1, -0.5, 0 and 0.08, flow along the top side, for $Pr = 11.6$. The Prandtl number effect was determined, for $Pr = 10.6$ and 12.6, only at R values of ± 2, ± 1, ± 0.5 and 0. The resulting buoyancy force, drag, pressure, heat-transfer and entrainment velocity parameters $I_w, f''(0), P(0), \phi'(0)$ and $f(\eta_e)$ are collected in Part A of Table 1. Also shown in Part C are the results obtained using the conventional linear approximation for the density difference in the buoyancy force. Convergence to the listed values was obtained by decreasing the step size

Table 1. Calculated values for both the isothermal and uniform flux horizontal plane flows
(A) Uniform temperature, $n = 0$

		$q = 1.894816$					$q = 1.582950$				
Pr	R	$f''(0)$	$P(0)$	$\phi'(0)$	$f(\eta_e)$	I_w	$f''(0)$	$P(0)$	$\phi'(0)$	$f(\eta_e)$	I_w
	−2.000	0.42369	−1.88908	−1.24856	0.27868	1.88908	0.32702	−1.32297	−1.14721	0.25671	1.32297
	−1.000	0.30818	−1.26582	−1.11850	0.24812	1.26582	0.26552	−1.01752	−1.06763	0.23797	1.01752
	−0.500	0.23319	−0.90451	−1.01298	0.22243	0.94051	0.22087	−0.81421	−1.00026	0.22152	0.81421
10.6	0.000	0.12525	−0.47260	−0.79006	0.15871	0.47260	0.14091	−0.51021	−0.83668	0.17314	0.51021
	0.500	0.13161	−0.27616	−0.88131	0.20750	−0.27616	0.14279	−0.30965	−0.90388	0.21120	−0.30965
	1.000	0.23728	−0.76695	−1.04749	0.23987	−0.76695	0.22317	−0.72663	−1.02238	0.23268	−0.72663
	2.000	0.37268	−1.48278	−1.20876	0.27398	−1.48278	0.30070	−1.12888	−1.12318	0.25387	−1.12888
	−16.000	1.18707	−7.44726	−1.82398	0.38956	7.44726	0.63256	−3.21252	−1.47908	0.31600	3.21252
	−8.000	0.82458	−4.60059	−1.61438	0.34448	4.60059	0.49889	−2.34718	−1.36600	0.29167	2.34718
	−4.000	0.57705	−2.88114	−1.43159	0.30493	2.88114	0.39534	−1.73006	−1.26312	0.26939	1.73006
	−2.000	0.40948	−1.85009	−1.27408	0.27046	1.85009	0.31607	−1.29564	−1.17067	0.24913	1.29564
	−1.000	0.29781	−1.23976	−1.14134	0.24081	1.23976	0.25661	−0.99653	−1.08945	0.23095	0.99653
	−0.500	0.22532	−0.88595	−1.03364	0.21589	0.88595	0.21344	−0.79745	−1.02069	0.21499	0.79745
11.6	0.000	0.12092	−0.46309	−0.80604	0.15414	0.46309	0.13608	−0.49986	−0.85365	0.16813	0.49986
	0.080	0.09542	−0.39077	−0.70082	0.10347	0.39077					
	0.301	0.05885	−0.00123	−0.74506	0.17815	−0.00123	0.07244	−0.02551	−0.79159	0.18760	−0.02551
	0.400	0.09739	−0.14638	−0.83771	0.19126	−0.14638	0.11027	−0.17709	−0.87169	0.19763	−0.17709
	0.500	0.12735	−0.27026	−0.89952	0.20134	−0.27026	0.13814	−0.30305	−0.92253	0.20494	−0.30305
	1.000	0.22943	−0.75093	−1.06900	0.23269	−0.75093	0.21577	−0.71149	−1.04336	0.22580	−0.71149
	2.000	0.36027	−1.45197	−1.23354	0.26588	−1.45197	0.20968	−1.10546	−1.14620	0.24637	−1.10546
	4.000	0.54142	−2.55477	−1.40869	0.30234	−2.55477	0.37924	−1.59956	−1.24991	0.26789	−1.59956
	8.000	0.79874	−4.33268	−1.60142	0.34301	−4.33268	0.48864	−2.25718	−1.35885	0.29086	−2.25716
	16.000	1.16833	−7.22727	−1.81665	0.38873	−7.22727	0.62604	−3.15037	−1.47520	0.31556	−3.15037
	−2.000	0.39686	−1.81523	−1.29786	0.26318	1.81523	0.30633	−1.27120	−1.19253	0.24242	1.27120
	−1.000	0.28860	−1.21645	−1.16262	0.23433	1.21645	0.24869	−0.97776	−1.10978	0.22473	0.97776
	−0.500	0.21832	−0.86935	−1.05288	0.21009	0.86935	0.20684	−0.78246	−1.03972	0.20921	0.78246
12.6	0.000	0.11708	−0.45456	−0.82092	0.15007	0.45456	0.13180	−0.49061	−0.86946	0.16368	0.49061
	0.500	0.12355	−0.26500	−0.91647	0.19589	−0.26500	0.13401	−0.29716	−0.93990	0.19940	−0.29716
	1.000	0.22244	−0.73661	−1.08904	0.22640	−0.73661	0.20918	−0.69797	−1.02689	0.21971	−0.69797
	2.000	0.34924	−1.42443	−1.25661	0.25871	−1.42443	0.28177	−1.08452	−1.16763	0.23972	−1.08452

(B) Uniform flux, $n = 2/(5+q)$

		$q = 1.894816, n = 0.290073$					$q = 1.582950, n = 0.303815$				
Pr	R	$f''(0)$	$P(0)$	$\phi'(0)$	$f(\eta_e)$	I_w	$f''(0)$	$P(0)$	$\phi'(0)$	$f(\eta_e)$	I_w
10.6	0.0	0.13638	−0.40244	−0.98448	0.12764	0.40244	0.15035	−0.43733	−1.04569	0.14156	0.43733
11.6	0.0	0.13157	−0.39438	−1.00503	0.12394	0.39438	0.14509	−0.42852	−1.06648	0.13744	0.42852
12.6	0.0	0.12730	−0.38716	−1.02325	0.12065	0.38716	0.14043	−0.42063	−1.08584	0.13378	0.42063

(C) Conventional buoyancy force approximation

	Uniform temperature, $n = 0$					Uniform flux, $n = 1/3$				
Pr	$f''(0)$	$P(0)$	$\phi'(0)$	$f(\eta_e)$	I_w	$f''(0)$	$P(0)$	$\phi'(0)$	$f(\eta_e)$	I_w
10.6	0.18741	−0.61747	−0.95575	0.21484	0.61747	0.19198	−0.53937	−1.19988	0.18301	0.53937
11.6	0.18115	−0.60468	−0.97531	0.20850	0.60468	0.18542	−0.52829	−1.22388	0.17759	0.52829
12.6	0.17558	−0.59326	−0.99353	0.20288	0.59326	0.17960	−0.51837	−1.24623	0.17278	0.51837

and increasing the region of integration until there was no further change in sixth decimal place.

The variation of $f''(0)$, $\phi'(0)$, I_w and $f(\eta_e)$ with R are also shown in Fig. 2 for $Pr = 11.6$ and $q(s,p) = q(0,1) = 1.894816$ and 1.589250. All curves are similar in that they approach zero rapidly in the region $0 < R < 0.5$. The tendency towards convective inversion is seen clearly in the plot of I_w vs R. The positive and negative ranges of R are separated by the region of buoyancy force reversal as indicated by change in sign of I_w. The break in the I_w curves in the region $0.08 < R < 0.301$ results from lack of numerical convergence in the region of small positive I_w. In this region buoyancy force reversal occurs in the outer part of the boundary region. The Prandtl number effect is seen from values in Part A of Table 1 to be quite small, a few percent.

For $Pr = 11.6$ and $q(s,p) = q(0,1) = 1.894816$, the tangential component of velocity f; the pressure P and the temperature ϕ are shown in Figs. 3–5 respectively, for various values of R. The weakening of the flow, f', in the range $0 < R < 0.5$, is seen in Fig. 3. At large $|R|$ the positive and negative R curves merge. The difference between f' at the peak, for $R = \pm 1$, is only 8%. This reduces to 2% for $R = \pm 4$. For ± 16 they have practically merged, the difference is less than 1%. Perhaps the most revealing of these results is the pressure P, plotted in Fig. 5. It is generally negative, but less so in the region $0 < R < 0.5$ where I_w approaches 0. Another effect is the further penetration outward of the temperature field in Fig. 5 and the resulting decreasing temperature gradient at the surface as R approaches 0. Each of these distributions is seen to merge at large $|R|$. However, the difference between the positive and negative values of R are on-flow on the lower and upper sides, respectively. This may be seen by reference again to the specific circumstance shown in Fig. 1.

CALCULATIONS FOR A SURFACE DISSIPATING A UNIFORM HEAT FLUX

For a uniform flux boundary condition the surface temperature was seen above to slowly increase downstream according to $d = (t_0 - t_\infty) = Nx^n$, where $n = 2/(q+5)$. Now, a necessary condition for a similarity solution of (22), so that, for example, $\varphi = \varphi(\eta)$, is that W does not depend on x. Thus, R, in (25), may not depend on x. A sufficient condition for this is $t_\infty = t_m(s,p)$, or $R = 0$. That is, the ambient medium is at the extremum temperature condition for the s and p levels which pertain there. For this condition, and for an imposed uniform surface heat flux, the equations (21)–(23) become

$$(q+5)f''' + 5(q+3)f''f - 5(q+1)f'^2 + 2P'\eta - \frac{2(3q-5)}{5}P = 0 \quad (34)$$

$$P' = W = \phi^q \quad (35)$$

$$(q+5)\varphi'' + Pr[5(q+3)\varphi' f - 10\varphi f'] = 0 \quad (36)$$

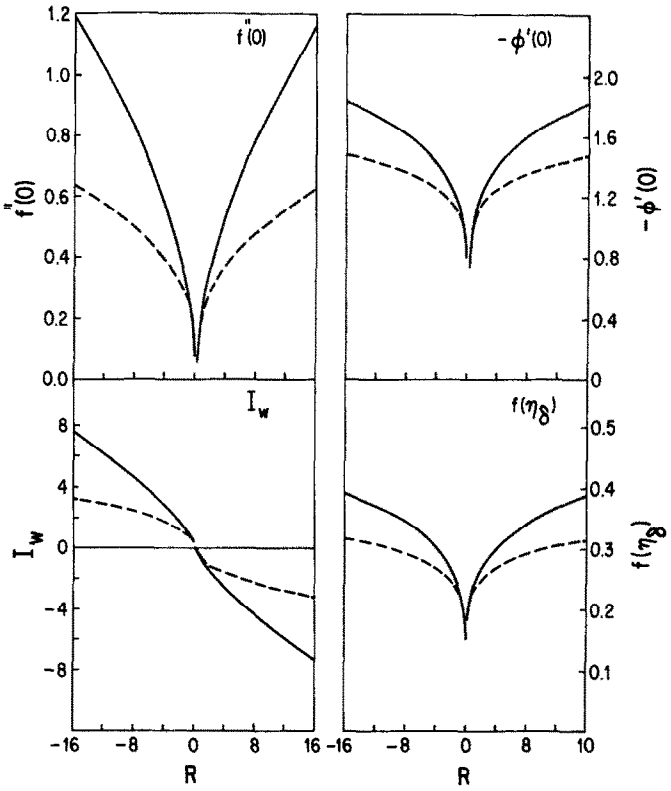

FIG. 2. Heat transfer $\phi'(0)$, drag $f''(0)$, mass flow rate $f(\eta_e)$ and net buoyancy I_w, over a range of R for an isothermal surface for $Pr = 11.6$ and —— $q = 1.894816$; - - - - - $q = 1.582950$.

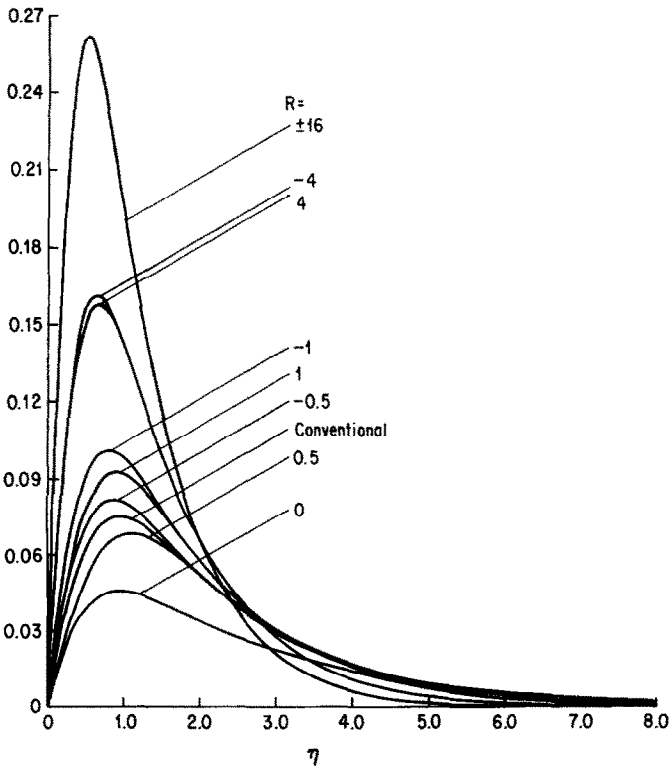

FIG. 3. Tangential component of velocity across the boundary region for an isothermal surface over a range of R for $Pr = 11.6$ and $q = 1.894816$. Values of R are shown on the curves.

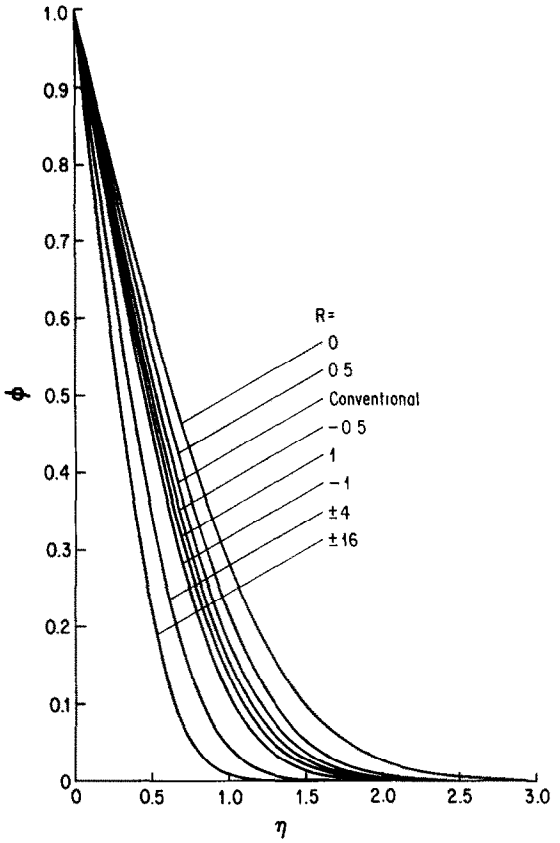

FIG. 4. Temperature distribution across the boundary region. Conditions same as in Fig. 3. Values of R are shown on curves.

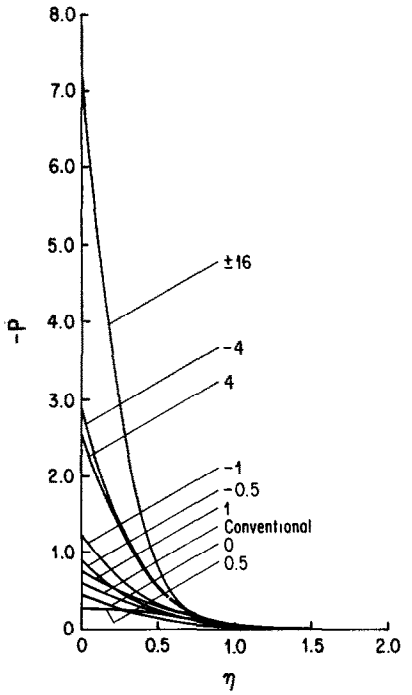

FIG. 5. Motion pressure distribution across the boundary region. Conditions same as in Fig. 3. Values of R are shown on curves.

$$f(0) = f'(0) = 1 - \varphi(0) = \varphi(\infty) = f'(\infty) = P(\infty) = 0. \quad (37)$$

The Grashof number is as defined in (20) and

$$N = \left(\left\{ \frac{q''}{k[-\phi'(0)]} \right\}^5 \frac{5\nu^2}{g\alpha} \right)^{1/(q+5)}. \quad (38)$$

The physical circumstance considered here may also be visualized on Fig. 1. Recall that $t_\infty = t_m$, $R = 0$. Since $t_0 > t_\infty = t_m$ for heat addition, the buoyancy force is inevitably up. Therefore, there will be on flow to the surface only on the upper side. Thus, the solution applies only there. Should the heat flux be negative as for an energy sink, due, for example, to radiation loss, the solution applies to flow on the lower side. Equations (34)–(36) were solved for $Pr = 10.6$, 11.6, and 12.6 for $q = 1.894816$ and 1.58295. The resulting buoyancy force, drag, heat-transfer and entrainment velocity parameters are collected in Part B of Table 1, together with the conventional results, for $q = 1$ in this formulation, in Part C. The results and the Prandtl number effect are seen to be similar to those at $R = 0$ for the isothermal surface condition, $n = 0$.

ANALYSIS OF AXISYMMETRIC FLOW

Axisymmetric flow on horizontal discs has been considered by Rotem [6], Rotem and Claassen [4] and by Blanc and Gebhart [9] for the conventional buoyancy force approximation. Such flows may arise in fluids adjacent to a horizontal surface when the temperature difference causing the buoyancy force is radially symmetric about a point on the surface. The resulting flow is subject to boundary-layer analysis when the spatial configuration of the temperature field generates, through the buoyancy force, a flow outward from the region of symmetry. Under this condition, the boundary-layer equations, without the usual buoyancy force approximation are:

$$u\frac{\partial u}{\partial x} + v\frac{\partial u}{\partial y} = \nu\frac{\partial^2 u}{\partial y^2} - \frac{1}{\rho}\frac{\partial p_m}{\partial x} \quad (39)$$

$$0 = -\frac{1}{\rho}\frac{\partial p_m}{\partial y} + g\frac{(\rho_\infty - \rho)}{\rho} \quad (40)$$

$$u\frac{\partial t}{\partial x} + v\frac{\partial t}{\partial y} = \frac{k}{\rho c_p}\frac{\partial^2 t}{\partial y^2} \quad (41)$$

$$\frac{\partial}{\partial x}(ux) + \frac{\partial}{\partial y}(vx) = 0. \quad (42)$$

Here x is distance measured in radial direction and other notation is as before for plane flow. The continuity equation is satisfied by the use of Stokes stream function ψ, defined as

$$u = \frac{1}{x}\frac{\partial \psi}{\partial y}, \quad v = -\frac{1}{x}\frac{\partial \psi}{\partial x}. \quad (43)$$

Following the procedure outlined above, for plane

Table 2. Calculated values for both the isothermal and uniform flux horizontal circular disc flows
(A) Uniform temperature, $n = 0$

		$q = 1.894816$					$q = 1.582950$				
Pr	R	$f''(0)$	$P(0)$	$\phi'(0)$	$f(\eta_e)$	I_w	$f''(0)$	$P(0)$	$\phi'(0)$	$f(\eta_e)$	I_w
	−2.000	0.28836	−1.54214	−1.52797	0.13053	1.54214	0.22260	−1.07995	−1.40399	0.12024	1.07995
	−1.000	0.20968	−1.03347	−1.36871	0.11622	1.03347	0.18070	−0.83067	−1.30653	0.11146	0.83067
	−0.500	0.15859	−0.73861	−1.23943	0.10419	0.73861	0.15027	−0.66477	−1.22400	0.10376	0.66477
10.6	0.000	0.08496	−0.38636	−0.96590	0.07440	0.38636	0.09567	−0.41694	−1.02317	0.08115	0.41694
	0.500	0.08991	−0.22511	−1.07938	0.09717	−0.22511	0.09752	−0.25244	−1.10690	0.09891	−0.25244
	1.000	0.16173	−0.62575	−1.28235	0.11230	−0.62575	0.15206	−0.59293	−1.25151	0.10898	−0.59293
	2.000	0.25386	−1.21007	−1.47957	0.12832	−1.21007	0.20480	−0.92132	−1.37477	0.11890	−0.92132
	−16.000	0.80791	−6.08042	−2.23183	0.18250	6.08042	0.43053	−2.62289	−1.80981	0.14804	−2.62289
	−8.000	0.56118	−3.75629	−1.97534	0.16138	3.75629	0.33953	−1.91640	−1.67144	0.13664	1.91640
	−4.000	0.39268	−2.35248	−1.75163	0.14285	2.3248	0.26905	−1.41257	−1.54552	0.12620	1.41257
	−2.000	0.27861	−1.51072	−1.55885	0.12671	1.51072	0.21508	−1.05792	−1.43237	0.11671	1.05792
	−1.000	0.20257	−1.01245	−1.39635	0.11282	1.01245	0.17458	−0.81375	−1.33293	0.10820	0.81375
	−0.500	0.15319	−0.72364	−1.26443	0.10115	0.72364	0.14517	−0.65126	−1.24871	0.10072	0.65126
11.6	0.000	0.08200	−0.37866	−0.98524	0.07227	0.37866	0.09237	−0.40858	−1.04371	0.07881	0.40858
	0.080	0.06455	−0.31993	−0.85579	0.04888	0.31993					
	0.301	0.04053	−0.00086	−0.91342	0.08344	−0.00086					
	0.400	0.06663	−0.11925	−1.02605	0.08958	−0.11925					
	0.500	0.08696	−0.22038	−1.10138	0.09431	−0.22038	0.09430	−0.24714	−1.12945	0.09600	−0.24714
	1.000	0.15632	−0.61285	−1.30836	0.10900	−0.61285	0.14696	−0.58074	−1.27687	0.10578	−0.58074
	2.000	0.24532	−1.18526	−1.50953	0.12455	−1.18526	0.19790	−0.90245	−1.40260	0.11541	−0.90245
	4.000	0.36858	−2.08567	−1.72378	0.14163	−2.08567	0.25816	−1.30589	−1.52946	0.12550	−1.30589
	8.000	0.54370	−3.53727	−1.95958	0.16069	−3.53727	0.33261	−1.84283	−1.66274	0.13626	−1.84283
	16.000	0.79524	−5.90058	−2.22292	0.18211	−5.90058	0.42611	−2.57208	−1.80510	0.14783	−2.57208
	−2.000	0.26994	−1.48259	−1.58762	0.12332	1.48259	0.20839	−1.03821	−1.45881	0.11359	1.03821
	−1.000	0.19625	−0.99364	−1.42209	0.10980	0.99364	0.16915	−0.79861	−1.35753	0.10530	0.79861
	−0.500	0.14840	−0.71024	−1.28772	0.09845	0.71024	0.16915	−0.63916	−1.27173	0.09803	0.63916
12.6	0.000	0.07939	−0.37176	−1.00325	0.07038	0.37176	0.08945	−0.40109	−1.06284	0.07674	0.40109
	0.500	0.08433	−0.21615	−1.12188	0.09178	−0.21615	0.09145	−0.24241	−1.15045	0.09342	−0.24241
	1.000	0.15151	−0.60132	−1.33259	0.10608	−0.60132	0.14243	−0.56984	−1.30050	0.10294	−0.56984
	2.000	0.23774	−1.16306	−1.53745	0.12122	−1.16306	0.19178	−0.88557	−1.42853	0.11232	−0.88557

(B) Uniform flux, $n = 2/(5+q)$

		$q = 1.894816, n = 0.290073$					$q = 1.582950, n = 0.303815$				
Pr	R	$f''(0)$	$P(0)$	$\phi'(0)$	$f(\eta_e)$	I_w	$f''(0)$	$P(0)$	$\phi'(0)$	$f(\eta_e)$	I_w
10.6	0.0	0.10294	−0.35096	−1.09789	0.06868	0.35096	0.11312	−0.38081	−1.16168	0.07533	0.38081
11.6	0.0	0.09930	−0.34400	−1.11963	0.06670	0.34400	0.10915	−0.37321	−1.18473	0.07316	0.37321
12.6	0.0	0.09608	−0.33775	−1.13988	0.06495	0.33775	0.10564	−0.36640	−1.20620	0.07123	0.36640

(C) Conventional buoyancy force approximation

	Uniform temperature, $n0$					Uniform flux, $n = 1/3$				
Pr	$f''(0)$	$P(0)$	$\phi'(0)$	$f(\eta_e)$	I_w	$f''(0)$	$P(0)$	$\phi'(0)$	$f(\eta_e)$	I_w
10.6	0.12760	−0.50399	−1.16974	0.10063	0.50399	0.14301	−0.46703	−1.32412	0.09478	0.46703
11.6	0.12339	−0.49369	−1.19341	0.09768	0.49369	0.13810	−0.45753	−1.35054	0.09200	0.45753
12.6	0.11947	−0.48448	−1.21545	0.09506	0.48448	0.13374	−0.44903	−1.37517	0.08953	0.44903

flow, it can be shown that the similarity transformation for the above set of equations is

$$\eta = \frac{y}{5x} G \tag{44}$$

$$\psi = vxGf \tag{45}$$

$$p_m = \frac{\rho v^2}{125x^2} G^4 P \tag{46}$$

$$\phi = \frac{t - t_\infty}{\mathrm{d}(x)} = \frac{t - t_\infty}{Nx^n} \tag{47}$$

where

$$G = 5\left(\frac{g\alpha|t_0 - t_\infty|^q x^3}{5v^2}\right)^{1/5} \tag{48}$$

$$R = \frac{t_m - t_\infty}{t_0 - t_\infty}. \tag{49}$$

With this transformation and the density equation (1), equations (39)–(41) become

$$f''' + (8+nq)ff'' - (2nq+1)f'^2 - \frac{nq-2}{5}\eta P' - \frac{4nq+2}{5} P = 0 \tag{50}$$

$$P = -\mathrm{sign}(g)[|\phi - R|^q - |R|^q] = -\mathrm{sign}(g)W \tag{51}$$

$$\phi'' + Pr[(nq+8)\phi' f - 5nf'\phi] = 0. \tag{52}$$

The boundary conditions at the surface and in the distant medium in transformed variables are

$$f(0) = f'(0) = 1 - \phi(0) = \phi(\infty) = f'(\infty) = P(\infty) = 0. \tag{53}$$

The limits on n for a physically meaningful flow are the same as for plane flow.

The above equations were solved for an isothermal ($n = 0$) surface condition for Prandtl numbers 10.6, 11.6 and 12.6 with $q = 1.894816$ and 1.58295. The resulting buoyancy force, drag, heat-transfer and entrainment velocity parameters are tabulated in Table 2. For a uniform flux boundary condition $n = 2/(q+5)$. Again $R = 0$. Results were obtained for $Pr = 10.6$, 11.6 and 12.6. These are also tabulated in Table 2. The results of conventional approximation, $q = 1$ when $R = 0$, are also shown for comparison. The temperature, velocity and pressure profiles in the boundary region are similar to those of the plane flow, as is the Prandtl number effect.

CONCLUSIONS

This is the first analysis of natural convection flows adjacent to horizontal surfaces in cold water, wherein a density extremum may occur. The use of the simple density relation for water, (1), has eliminated the need of any approximation in the buoyancy force term. Only two new parameters R and q arise. These determine the fundamental nature of the density field and the effects of the pressure and salinity levels, respectively.

Extensive calculations are presented for horizontal surfaces with both isothermal or uniform flux conditions. Wide ranges of Prandtl number, salinity and pressure levels, q, and temperature conditions R are considered. The conventional buoyancy force approximation is included in the present formulation by choosing $q = 1$ in those flows for which $R = 0$.

The parameter I_w determines the vigor of the flow and the condition for convective inversion. For flow over a horizontal surface, we find that $I_w \approx 0$ for $R \approx 0.301$. Thus, for an ice slab melting in water, this corresponds to an ambient temperature of $t_\infty \simeq 5.7°C$. In experiments with a vertical ice surface melting in water, Bendell and Gebhart [15] found flow reversal to occur between 5.5 and 5.6°C. A particular striking result is the sharp decrease in heat transfer in the region of density inversion. The effect of Prandtl number and q on heat transfer is small when $|R|$ is small, and it increases with an increase in R. No applicable experimental data are available to compare with our numerical results.

Acknowledgements—The authors wish to acknowledge support for this study by the National Science Foundation under grant ENG 75-2263. We would also like to acknowledge the expert efforts of Mrs. B. Boskat in the preparation of this manuscript.

REFERENCES

1. E. Schmidt, Schlierenaufnahmen des Temperaturfeldes in der Nahe warmebgebender Korper, *Forsch. Geb. Ingwes.* **3**, 181–189 (1932).
2. K. Stewartson, On free convection from a horizontal plate, *Z. Angew. Math. Phys.* **9a**, 276–281 (1958).
3. W. N. Gill, D. W. Zeh and E. del Casal, Free convection on a horizontal plate, *Z. Angew. Math. Phys.* **16**, 539–541 (1965).
4. Z. Rotem and L. Claassen, Free convection boundary-layer flow over horizontal plates and discs, *Can. J. Chem. Engng.* **47**, 461–468 (1969).
5. Z. Rotem and L. Claassen, Natural convection above unconfined horizontal surfaces, *J. Fluid Mech.* **38**, 173–192 (1969).
6. Z. Rotem, Contribution to the theory of free convection from horizontal plates, in *Proceedings of the First Canadian National Congress on Applied Mechanics*, Vol 2.
7. L. Pera and B. Gebhart, Natural convection boundary layer flow over horizontal and slightly inclined surfaces, *Int. J. Heat Mass Transfer* **16**, 1131–1146 (1973).
8. L. Pera and B. Gebhart, On the stability of natural convection boundary layer flow over horizontal and slightly inclined surfaces, *Int. J. Heat Mass Transfer* **16**, 1147–1163 (1973).
9. P. Blanc and B. Gebhart, Buoyancy induced flows adjacent to horizontal surfaces, in *Proceedings of the Fifth International Heat Transfer Conference*, Tokyo, Paper No. NC1.5, pp. 20–24 (1974).
10. B. Gebhart and J. C. Mollendorf, Buoyancy-induced flows in a liquid under conditions in which density extrema may arise, to be published.
11. B. Gebhart and J. C. Mollendorf, A new density relation for pure and saline water, to be published.
12. K. Fujino, E. L. Lewis and R. G. Perkin, The freezing point of sea water at pressures up to 100 bars, *J. Geophys. Res.* **79**, 1792–1797 (1974).
13. J. M. Dumoré, H. J. Merk and J. A. Prins, Heat Transfer from water to ice by thermal convection, *Nature* **172**, 460–461 (1953).
14. J. Schenk and F. A. M. Schenkels, Thermal free convection from an ice sphere in water, *Appl. Scient. Res.* **19**, 465–476 (1968).
15. M. S. Bendell and B. Gebhart, Heat transfer and ice melting in ambient water near its density extremum, *Int. J. Heat Mass Transfer* **19**, 1081–1087 (1976).

CONVECTION NATURELLE SUR DES SURFACES HORIZONTALES DANS L'EAU AU VOISINAGE DE L'EXTREMUM DE DENSITE

Résumé—On analyse la convection naturelle générée dans l'eau froide adjacente à une surface horizontale. Un traitement de région frontière est approprié à un large domaine de conditions lorsque la force de poussée est éloignée de la surface. Lorsque la configuration est axisymétrique par rapport à une normale à la surface, il existe un écoulement radial. Le régime de couche limite existe aussi quand la poussée d'Archimède est éloignée de la surface avec l'écoulement s'écartant de l'axe. Les deux types de convection naturelle sont considérés pour une température basse d'eau pure ou salée, lorsqu'un extrémum de densité existe dans le domaine considéré. Une nouvelle équation simple de densité donne une formulation compacte de transport à la fois pour l'écoulement de plan et de disque. Des solutions sont données pour des conditions réalistes de nombre de Prandtl et de température. On note des renversements de poussée et des conditions d'inversion de convection. Des tabulations détaillées des paramètres de transport sont incluses pour les deux cas de surface isotherme et de flux pariétal uniforme. Ces résultats sont comparés à ceux qui sont obtenus pour l'approximation classique des forces de poussée.

DURCH AUFTRIEB HERVOGERUFENE STRÖMUNGEN AN HORIZONTALEN FLÄCHEN IN WASSER NAHE SEINES DICHTEEXTREMUMS

Zusammenfassung—Es werden Strömungen untersucht, die in kaltem Wasser nahe einer horizontalen Fläche durch Auftrieb hervorgerufen werden. Eine Behandlung als Grenzschichtgebiet ist in einem weiten Bereich von Bedingungen angebracht, wenn der Netto-Effekte der Auftriebskraft von der Fläche weggerichtet ist. Dies ergibt eine Zuströmung an der Anströmkante einer ebenen Strömung, die auftreten kann, wenn die räumliche Anordnung der Auftriebskraft in zweidimensionalen kartesischen Koordinaten beschrieben werden kann. Eine radiale oder Scheiben-Strömung ergibt sich, wenn die Anordnung radial symmetrisch zu einer Flächennormalen ist. Ein Grenzschichtgebiet ergibt sich auch hier, wenn der Netto-Auftrieb von der Oberfläche weg und die Strömung von der Achse nach außen gerichtet ist. Beide Arten

von Strömungen durch thermischen Auftrieb werden in reinem oder salzigem Wasser bei niedriger Temperatur betrachtet, wobei ein Dichteextremum im Auftriebsgebiet vorliegen kann. Eine neue, sehr genaue und einfache Dichtegleichung ergibt eine kompakte Formulierung der Transports sowohl für ebene wie Scheibenströmungen. Für die Prandtl–Zahlen und Temperaturbedingungen, die normalerweise vorkommen, werden Lösungen angegeben. Auftriebsumkehr und Bedingungen für konvektive Inversion treten auf. Detaillierte Täbellen der Transportparameter sind beigefügt, sowohl für Randbedingungen mit isothermen Oberflächen wie für solche mit konstantes Wärmestromdichte. Die Ergebnisse werden mit jenen verglichen, die erzielt werden, wenn man die übliche Approximation der Auftriebskrafte benutzt.

ПОТОКИ, ВОЗНИКАЮЩИЕ У ГОРИЗОНТАЛЬНЫХ ПОВЕРХНОСТЕЙ В РЕЗУЛЬТАТЕ ДЕЙСТВИЯ АРХИМЕДОВЫХ СИЛ В ВОДЕ ВБЛИЗИ ЕЕ ЭКСТРЕМАЛЬНОЙ ПЛОТНОСТИ

Аннотация — Анализируются потоки, возникающие в холодной воде у горизонтальной поверхности в результате действия архимедовых сил. Приближение пограничного слоя можно использовать для широкого диапазона условий, когда суммарный эффект архимедовых сил сказывается вдали от поверхности. Это проявляется в натекании на переднюю кромку при плоскопараллельном течении, что может иметь место в случае, когда пространственная конфигурация подъёмной силы описывается в двумерной системе декартовых координат. Радиальное или дискообразное течение возникает в том случае, когда конфигурация является радиально симметричной относительно нормали к поверхности. Режим пограничного слоя возникает опять, когда суммарная подъёмная сила действует вдали от поверхности, а течение происходит наружу от оси. Рассматриваются оба вида тепловых свободноконвективных потоков, возникающих при низкой температуре в чистой или солёной воде, в которой экстремум плотности может иметь место в области действия архимедовых сил. Новое, довольно точное и простое, уравнение для плотности позволяет получить компактную формулировку переноса в случаях плоского и дискообразного течений. Приводятся решения для числа Прандтля и температурных условий, которые обычно встречаются на практике. Отмечается возникновение обращения подъёмных сил и условий конвективной инверсии. Приводятся подробные таблицы параметров переноса как для изотермических условий на поверхности, так и для случая однородного теплового потока на поверхности. Дано сравнение полученных результатов со случаем использования обычного архимедового приближения.